Shock and Vibration 19 (2012) 1267–1280
DOI 10.3233/SAV-2012-0669
IOS Press

Two-mode operation engine mount design for automotive applications

Reza Tikani[a], Nader Vahdati[b] and Saeed Ziaei-Rad[a,*]
[a]*Department of Mechanical Engineering, Isfahan University of Technology, Isfahan, Iran*
[b]*Department of Mechanical Engineering, The Petroleum Institute, Abu Dhabi, UAE*

Received 29 November 2010
Revised 22 November 2011

Abstract. Hydraulic engine mounts are applied to the automotive applications to isolate the chassis from the high frequency noise and vibration generated by the engine as well as to limit the engine shake motions resulting at low frequencies. In this paper, a new hydraulic engine mount with a controllable inertia track profile is proposed and its dynamic behavior is investigated. The profile of the inertia track is varied by applying a controlled force to a cylindrical rubber disk, placed in the inertia track. This design provides a hydraulic engine mount design with an adjustable notch frequency location and also damping characteristics in shake motions. By using a simple control strategy, the efficiency of the proposed hydraulic engine mount in two-mode operation meaning isolating mode in the highway driving condition and damping mode in the shock motions, is investigated.

Keywords: Hydraulic engine mounts, variable notch frequency, semi-active mount, NVH

1. Introduction

Engine mounts need to perform three tasks:

(1) Support engine weight
(2) Control cabin noise and vibrations
(3) And limit engine motion in the presence of large shocks

Most engine mounts, being elastomeric or hydraulic, perform the first task properly. Both elastomeric and hydraulic engine mounts do provide cabin noise and vibration reduction with a difference that hydraulic engine mounts provide an extra noise and vibration reduction at a frequency called “notch frequency”. The trouble with hydraulic engine mount is that the notch frequency is tuned to a particular frequency and thus if engine RPM changes drastically, the noise and vibration reduction will not be optimum anymore.

In fixed and rotary wing applications, the variation in engine RPM, during cruise condition, is very small, whereas in the automotive applications, the engine RPM varies greatly. To effectively use hydraulic engine mounts in automotive applications, an adjustable notch frequency hydraulic engine mount is definitely required. Another difference between aerospace and automotive applications is that the shock and large motions rarely occur in aerospace applications.

To solve the engine RPM variation problem, many researchers have resorted to semi-active hydraulic engine mounts to vary the notch frequency location in order to match it with the change in the engine RPM. Compared

*Corresponding author: Saeed Ziaei-Rad, Department of Mechanical Engineering, Isfahan University of Technology, Isfahan 84156-83111, Iran. Tel.: +98 311 391 5244; Fax: +98 311 391 2628; E-mail: szrad@cc.iut.ac.ir.

ISSN 1070-9622/12/$27.50

with the passive engine mounts, the semi-active and active engine mounts have higher cost, weight and energy consumption.

For aerospace applications, the existing semi-active hydraulic engine mount designs are sufficient to respond to the need for engine RPM variation [1] but for automotive applications, there is a 3$^{\mathrm{rd}}$ task for the engine mounts to perform, and that is to provide large damping, when large engine motions and shocks are involved.

Extensive literature review was conducted to see if a hydraulic engine mount that satisfies the above three tasks has been proposed or reported.

- Hydraulic mounts with decoupler [2,3] (solves task 3 but the notch frequency is not variable)
- Magneto-Rheological(MR) and Electro-Rheological(ER) fluid mounts solve tasks 1 and 3. However, due to high viscosity and flow losses of MR-fluids, the notch depth is shallow and notch adjustability is not there [4,5]

To achieve best reduction in cabin noise and vibration, researchers have focused on semi-active hydraulic engine mounts that adjust the mount notch frequency by changing the mount parameters [6]. There are several ways to change the notch frequency location. Some of these ways are based on using smart materials such as electro-rheological fluids [7–9], magneto-rheological fluids [5,10,11] and shape memory alloys [12] in the hydraulic engine mount design. In some other works, different mechanisms [6,13–15] has been utilized to change the engine mount dynamic properties.

There are some advantages and some drawbacks in each design. Some of these ways are expensive such as using MR and ER fluids, and some of them are not effective in a wide range of frequencies [6,16]. Also, in most of current ways, the notch depth reduced during adjusting the notch frequency location [17]. For example, in the mounts that are filled with MR fluids because of high viscosity of these fluids usually the notch depth is not deep enough and good reduction in the vibration isolation cannot be achieved. There is an interesting design by Barber and Carlson [4] that shows the good performance of using MR fluids in damping mode, but there is not a deep notch for isolation purposes. Variable volumetric stiffness fluid mount is another approach to control the notch frequency location, but it cannot be useful in a wide range of frequencies. Vahdati and Ahmadian [6] have proposed a variable volumetric stiffness fluid mount that can change the notch frequency in the range of 25 to 37 Hz. Changing inertia track length and diameter is another common way to change the notch frequency location. Foumani et al. [13] have presented a mechanism that continuously changes the inertia track length in order to be effective in low-frequency, high-amplitude vibrations. The effect of using multiple inertia tracks in the hydraulic engine mounts was investigated by Zhang and Shangguan [15]. They have shown the dynamic stiffness and loss angle of a hydraulic engine mount with 3 different inertia tracks. Controllable inertia track area was the subject of the work carried out by Truong and Ahn [14]. In their design, the area of the inertia track is controlled in order to change the dynamic stiffness in low frequencies.

In this paper, a new hydraulic engine mount design is presented that performs all the above three tasks with an adjustable notch frequency. The new mount design is simple and effective, for control of cabin noise and vibrations, and limiting shock induced engine motion, in the automotive applications. The new hydraulic engine mount design is capable of changing the notch frequency location during the highway driving conditions by controlling the profile of the inertia track. The flow loss in the new design is smaller than when one changes the length or diameter of the inertia track, so the deeper notch and better isolation will be obtained. Also, the design will perform in the low-frequency, high amplitude vibrations as a damper and in the high-frequency, low amplitude vibration as a vibration absorber. The latter can be achieved by changing the inertia track profile with a simple control strategy.

2. Mathematical model of new hydraulic engine mount

As mentioned in the previous section, the main idea of this study, i.e. working in the two mode operation, is based on adjusting the inertia track profile. The new semi-active fluid engine mount is depicted in Fig. 1. The mount consists of a rubber structure with two, top and bottom fluid chambers and a cylindrical rubber disk that sits in the inertia track and controls the inertia track profile. A linear solenoid actuator applies force to compress the cylindrical rubber disk in the inertia track. By applying this force, the inertia track properties will be varied.

The bond graph model of the semi-active mount is illustrated in Fig. 2. The state space equations, from the bond graph model, can be derived as,

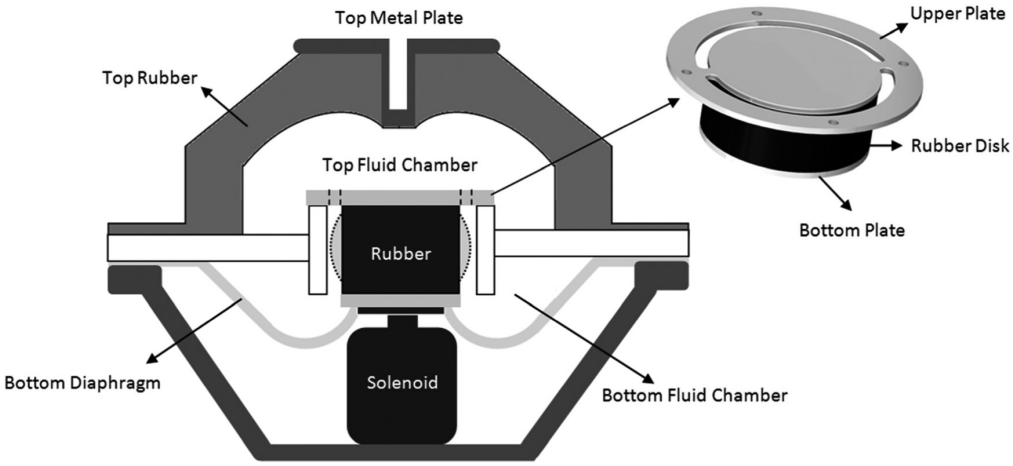

Fig. 1. Proposed semi-active hydraulic mount.

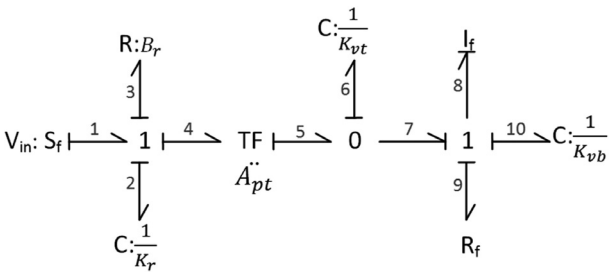

Fig. 2. Bond graph model of the semi-active mount.

$$\dot{q}_2 = V_{in} \tag{1}$$

$$\dot{q}_6 = A_{pt} V_{in} - \frac{P_8}{I_8} \tag{2}$$

$$\dot{P}_8 = \frac{q_6}{C_6} - R_9 \frac{P_8}{I_8} - \frac{q_{10}}{C_{10}} \tag{3}$$

$$\dot{q}_{10} = \frac{P_8}{I_8} \tag{4}$$

The input force (effort in bond 1) is given by

$$F_{in} = \frac{q_2}{C_2} + R_3 V_{in} + A_{pt} \frac{q_6}{C_6} \tag{5}$$

The ratio of the transmitted force by the input displacement applied to the mount is called dynamic stiffness ($K^* = F_{in}/X_{in}$) [18].

In the above state space equations $\dot{q}_2$, $\dot{q}_6$ and $\dot{q}_{10}$ are the generalized displacement variables, and $\dot{P}_8$ is the momentum variable. The state space variables are defined as:

- q_2 Relative motion across the mount
- q_6 Top chamber change in volume
- q_{10} Bottom chamber change in volume
- P_8 Time integral of the pressure drop in the inertia track (pressure momentum)

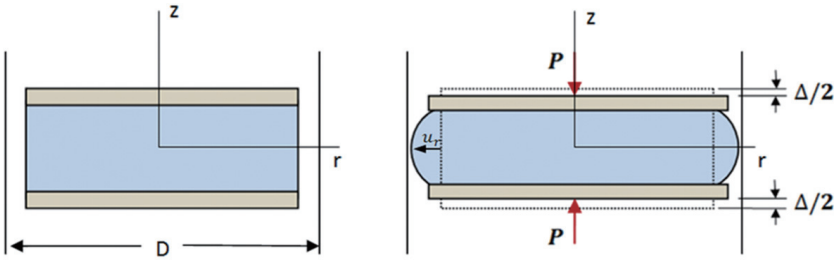

Fig. 3. Undeformed and deformed configurations of a bonded elastic layer.

To simulate the model of Fig. 2, a MATLAB program was developed in which the above state space equations with the following baseline parameters were used.

V_{in}	velocity across the mount, m/s
A_{pt}	effective area of the top metal, 0.0025 m^2
I_f	fluid inertia in the inertia track, same as I_8, Ns^2 /m^5
R_f	inertia track flow resistance, same as R_9, Ns/m^5
K_r	axial stiffness of top rubber ($C_2 = 1/K_r$), 2.25e5 N/m
B_r	damping component of top rubber ($R_3 = B_r$), 50 Ns/m
K_{vt}	top chamber volumetric stiffness ($C_6 = 1/K_{vt}$), 3.33e10 N/m^5
K_{vb}	bottom chamber volumetric stiffness ($C_{10} = 1/K_{vb}$) 3.84e8 N/m^5

The fluid inertia (I_f) and inertia track flow resistance (R_f) are variable parameters and will be calculated in the next section depending on the inertia track profile. These parameters must be calculated by numerical integration methods.

3. Fluid inertia and resistance calculation

The linear actuator can change the rubber shape or contour of the solid rubber disk and here in this section, the relation between applied force and varied shape and also its effect on the fluid inertia and fluid resistance will be investigated.

The effective modulus of the bonded rubber layer under its deformation state may be determined whenever the stress distributions are determined. Effective compression modulus, E_c, of a bonded elastic layer (Fig. 3) can be obtained from the ratio of nominal compressive stress, defined as the ratio of applied axial load (P) to the undeformed horizontal sectional area (A) of the layer, to nominal compressive strain, defined as the ratio of total compression of the layer, Δ, to its initial thickness. Thus, for the effective compression modulus, E_c, one has [19]

$$E_c = \frac{P}{A\epsilon_c} \tag{6}$$

Where $\varepsilon_c = \frac{\Delta}{t}$ and t is the thickness of rubber layer.

The effective compression modulus, E_c, can obtained as [20]

$$E_c = \alpha - \frac{\lambda^2}{\alpha(\beta_{r0}R)\frac{I_0(\beta_{r0}R)}{2I_1(\beta_{r0}R)} - \mu} \tag{7}$$

In Eq. (7), $\alpha = 2\mu + \lambda$ where μ and λ are Lame's constants and are equal to 0.386 MPa and 1489.6 MPa, respectively. The symbols $I_0(\beta_{r0}R)$ and $I_1(\beta_{r0}R)$ are the modified Bessel function of the first kind, where R is the disk radius and $\beta_{r0}^2 = \frac{12\mu}{\alpha t^2}$.

The relationship between applied force and deformation in vertical direction can be calculated by plugging Eq. (7) into Eq. (6).

Displacement of lateral faces of the layer can be determined for the cylindrical rubber disk as,

$$u_r = \frac{3}{2} a_{r0} I_1(\beta_{r0} R) \left(1 - \frac{4z^2}{t^2}\right) \tag{8}$$

Where a_{r0} is a constant and can be expressed as,

$$a_{r0} = \frac{\lambda \Delta}{\alpha t} \frac{1}{\beta_{r0} I_0(\beta_{r0} R) - \frac{2\mu}{\alpha R} I_1(\beta_{r0} R)} \tag{9}$$

The equation used to calculate fluid inertia or fluid inductance in the inertia track is [21]

$$I_f = \frac{\rho L}{A_i} \tag{10}$$

Where ρ, L and A_i are fluid density (1765 kg/m^3), length and cross section area of the inertia track respectively.

Since the cross section area is not a constant, the fluid inertia is determined via the following integral equation.

$$I_f = \int_{-t/2}^{t/2} \frac{\rho dz}{\pi \left(\left(\frac{D}{2}\right)^2 - u_r^2 \right)} \tag{11}$$

Where D is the inertia track diameter.

The fluid resistance in the annular section with outer diameter of d and symmetrical clearance of b is [21]

$$R_f = \frac{8\mu L}{\pi d b^3 \left(1 - \frac{b}{d}\right)} \tag{12}$$

Similar to the fluid inertia, since the symmetrical clearance is not a constant in the length of the inertia track, the fluid resistance can be expressed as

$$R_f = \int_{-t/2}^{t/2} \frac{8\mu dz}{\pi D \left(\frac{D}{2} - u_r\right)^3 \left(1 - \frac{\frac{D}{2} - u_r}{D}\right)} \tag{13}$$

The parameter u_r in Eqs (11) and (13) is a function of z, and can be obtained from Eq. (8). Equations (11) and (13) are numerically evaluated by the developed MATLAB code.

By applying the actuator force to the cylindrical rubber disk, the shape of the rubber and therefore the fluid inertia and fluid resistance will change. Change in these variables will cause significant changes in dynamic stiffness and notch frequency of the mount.

4. Calculating optimum values by using genetic algorithm

In automotive applications, for an internal combustion engine, there exist two basic dynamic disturbances: primary disturbances (the inertia forces and torques caused by the rotating and reciprocating parts such as piston, connecting rod, and crank) and secondary disturbances (the firing pulses due to the explosion of the fuel in the cylinders) [22].

The engine speed of 4-cylinder passenger car during the highway driving condition varies from one engine manufacturer to the other, but it is usually in the range of 2000 rpm to 2500 rpm. For example, for a typical 4-cylinder car with the engine speed of 2400 rpm (40 Hz) at the highway driving condition, the rotating and reciprocating parts of the engine such as the piston, the connecting rod, and the crank rotate at 40 Hz but the cylinders fire at twice the speed of the engine, namely 80 Hz.

Engine manufacturers make great attempts to balance the rotating and reciprocating parts of an engine during manufacturing and minimizing the vibration induced due to the primary disturbances [23]. However, the vibration created by the firing of the cylinders can affect the vehicle compartments and it is highly desirable to design the fluid mounts such that they can eliminate the effect of secondary disturbances (firing pulses).

In this paper, only secondary disturbances are considered and optimum values of rubber length and diameter are obtained for a typical 4-cylinder car with the engine speed of 2400 rpm (80 Hz) during highway driving condition. It should be noticed that in the current design, the notch frequency of the mount in the passive mode is intentionally

designed to occur in the frequency of 90 Hz and vibration isolation will be provided in the operating frequency range of 70 to 90 Hz continuously.

To obtain optimum values of rubber length and diameter, the genetic optimization algorithm is applied. The fitness function is defined to set the applied force in Eq. (6) to minimum value and also to have notch frequency at 90 Hz without applying any force. Equation (14) explained the fitness function and the lower and upper bonds of the variables.

$$\textit{Fitness Function} = w_1(f_{notch} - 90)^2 + w_2\left(1 - \frac{P}{P_a}\right)^2 \tag{14}$$

$$0.02 \leqslant L \leqslant 0.05\ m$$

$$0.01 \leqslant D \leqslant 0.05\ m$$

$$0 \leqslant \Delta \leqslant 0.005\ m$$

Where w_1 and w_2 are weighting factors and are assumed equal to 1. The variable P is the applied force to the rubber disk and can be calculated from Eq. (6) where P_a is the maximum force that the actuator can applied to the rubber disk in the mode of 100% solenoid duty cycle.

It was shown by Vahdati [18] that the notch and peak frequency locations are weakly sensitive to damping; so, to find f_{notch}, all the damping factors in Eqs (1) to (5) are set to zero. Therefore, if the numerator of K^* is set to zero, the following notch frequency will be obtained.

$$f_{notch} = \frac{1}{2\pi}\sqrt{\frac{A_p^2 K_{vt} K_{vb} + K_r(K_{vt} + K_{vb})}{I_f(K_r + A_p^2 K_{vt})}} \tag{15}$$

The optimum values are calculated by genetic algorithm in MATLAB. The results for the fitness function of Eq. (13) is

$$L = 0.0205\ m$$

$$D = 0.0494\ m$$

$$\Delta = 0.0043\ m$$

In the next session by using MATLAB program, the dynamic stiffness of the hydraulic mount with the preceding baseline parameters has been simulated.

5. Dynamic response of proposed hydraulic engine mount

The dynamic stiffness of the hydraulic engine mount is obtained in this section to evaluate dynamic characteristics of the mount. Figure 4 illustrates the dynamic stiffness of the mount under the conditions that the inertia track flow resistance is constant and the only change in the mount parameters is increase in fluid inertia due to change in inertia track profile. By increasing the fluid inertia, the notch frequency goes to the lower frequencies (this phenomenon also can be found by Eq. (15)) and the notch depth will be deeper. On the other hand, by changing the inertia track profile, the resistance will be increased too and it causes a reduction in the notch depth. As a result of both parameters, the notch depth remains constant in a wide range of frequency and it promises a good isolation.

Figure 5 illustrates the dynamic stiffness of hydraulic mount versus frequency that changes by applying force to the rubber disk in the inertia track. Figure 5 clearly shows the wide range of controllable notch frequency. In the case of shake motion (sudden acceleration and deceleration, braking and riding on uneven roads) the hydraulic engine mount can be converted to a damper by applying required force to the rubber disk. Figure 6 shows the required force versus the notch frequency of the hydraulic mount. From Fig. 6, one can find the required force which is needed to change the inertia track profile and thus adjusts the notch frequency to the desired frequency. Figure 7 shows the corresponding rubber disk compression versus the notch frequency of the mount. Using these two figures, one can

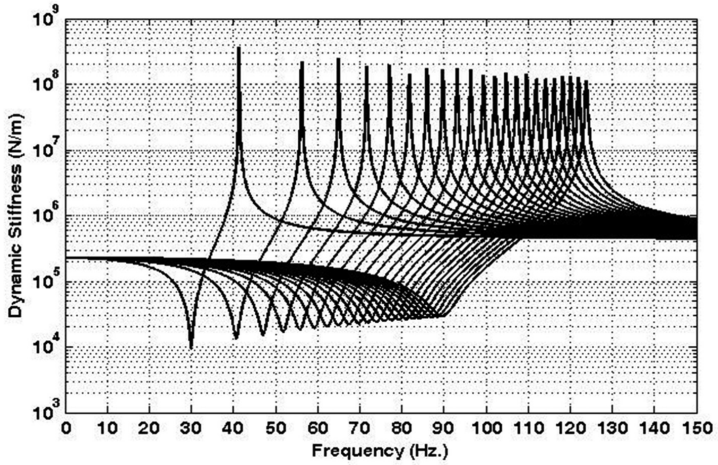

Fig. 4. Dynamic stiffness of the hydraulic mount when resistance is constant.

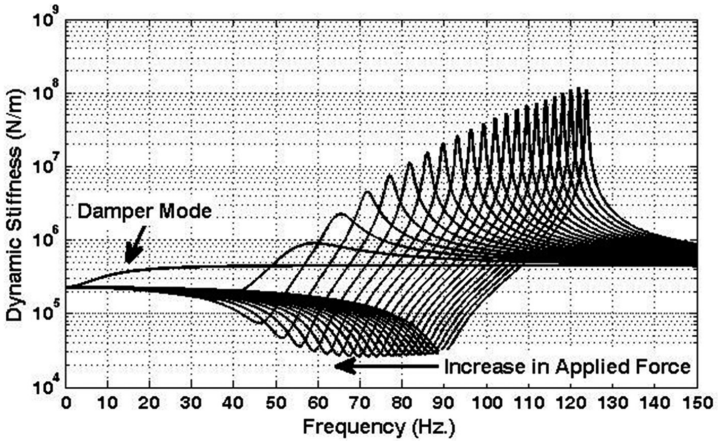

Fig. 5. Dynamic stiffness of the hydraulic engine mount.

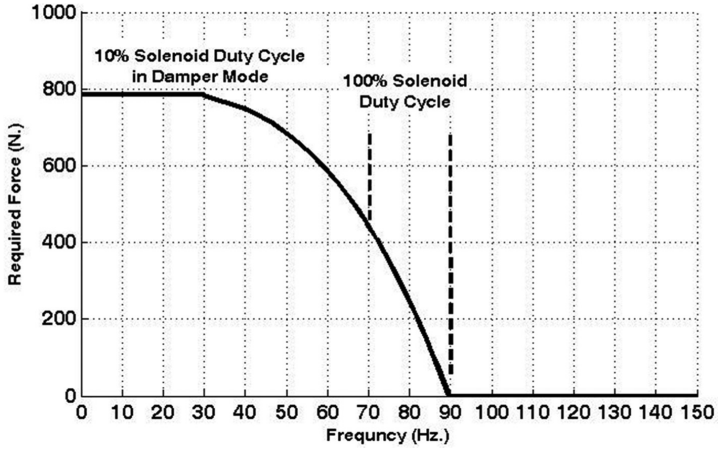

Fig. 6. Required force versus notch frequency.

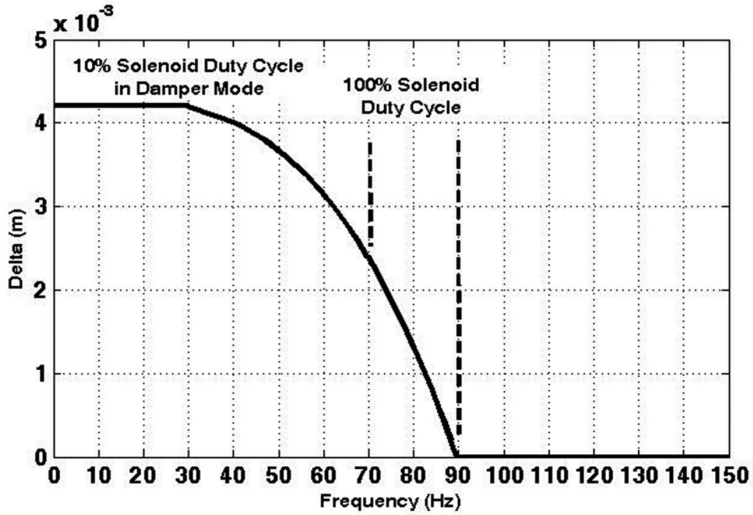

Fig. 7. Rubber compression versus notch frequency.

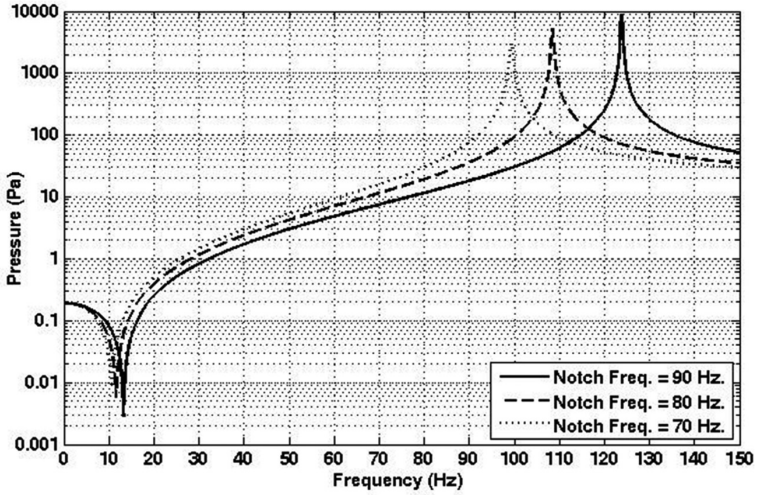

Fig. 8. Upper chamber pressure in the hydraulic engine mount.

easily select the proper solenoid actuator. Finally, these two figures will be used as a look-up table in the control strategy to find out the required power needs for the solenoid as will be described in the following sections.

Figures 8 and 9 show the magnitude of the dynamic pressure in the top and bottom chambers of the hydraulic engine mount when the input displacement magnitude is 10^{-3} meter. The dynamic pressure in the chambers when the hydraulic engine mount is working at the 80 Hz notch frequency is 12.26 Pa in the upper chamber and 0.3977 Pa in the bottom chamber. By using these figures, one can find the frequencies in which the maximum dynamic pressure in the chambers happens.

To avoid resonance characteristics in high speeds, one can change the isolation mode to the lower notch frequency isolation mode. For example, there is obvious in Fig. 5, and also in Figs 8 and 9, when the notch frequency is 90 Hz, the peak frequency of dynamic pressure and dynamic stiffness will be near 124 Hz. In this case if the engine's speed reaches to this frequency, it will go to resonance. To eliminate resonance, one can change the isolation mode to the mode that notch frequency is equal to 70 Hz. In this way, the dynamic stiffness and chamber's pressure will be reduced effectively.

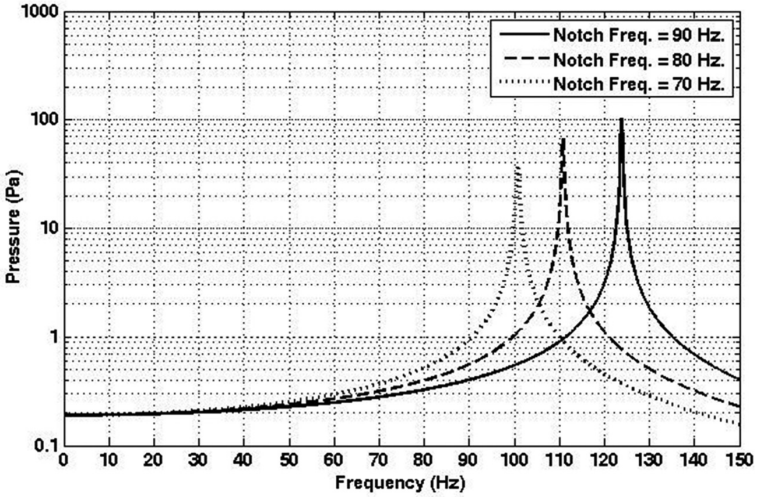

Fig. 9. Bottom chamber pressure in the hydraulic engine mount.

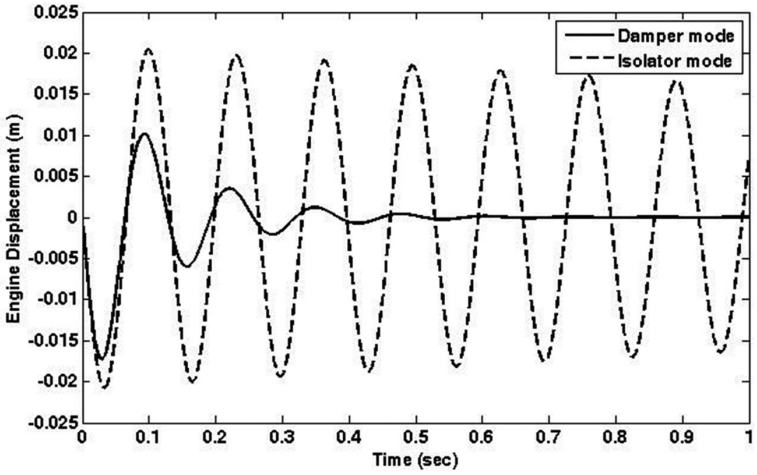

Fig. 10. Engine displacement with respect to an initial velocity of engine.

6. Numerical simulations in damper mode

As discussed in previous sections, the best vibration isolation response for the mount can be obtained by adjusting the applied force. The dynamic response of the mount clearly indicates this fact. In this section, the simulation results of the mount in the case of shake motion are discussed. As shake motion happens regarding to sudden acceleration and deceleration, braking and riding on uneven roads, the time domain response of the mount when engine experience an initial velocity is considered here.

Figure 10 displays the vibration of an engine with the mass of 100 kg with the initial velocity of 1 m/s in two different modes. The value of as shown in Fig. 7 for the damper mode is 0.0042 m.

7. Actuator selection considerations

Stroke and force are two important parameters in selection of actuators in this design. Additionally, the power of the selected actuator must be in the range of automotive electrical devices. The size and the time response of

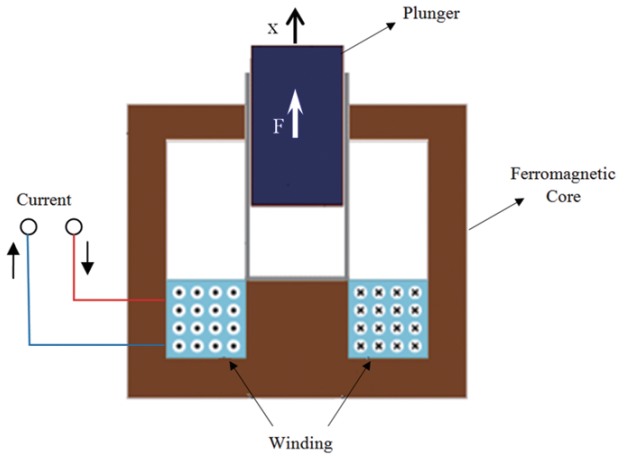

Fig. 11. Linear solenoid actuator schematic.

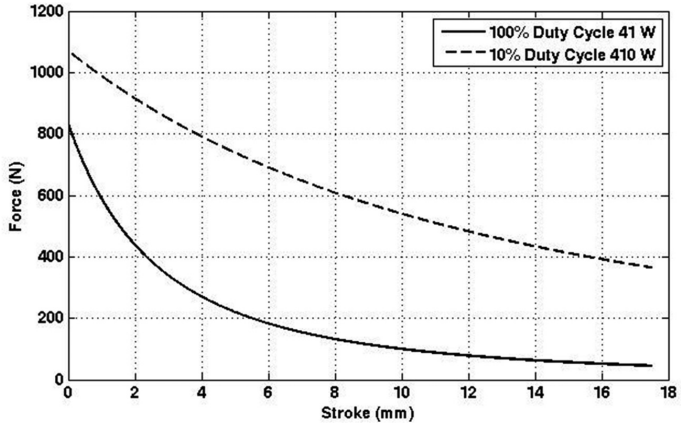

Fig. 12. Force-stroke diagram for a commercial linear solenoid.

the actuator are also significant in selection of actuator type but unlike active engine mount actuators the frequency range of the actuator are not important in this design. The linear solenoids can meet these criteria.

Figure 11 illustrates the schematic model of a solenoid. By applying proper current, the plunger will be moved by electromagnetic force. The electromagnetic force is related to the solenoid current and inductance by

$$F = \frac{1}{2} i^2 \frac{\partial L(x)}{\partial x} \tag{16}$$

The inductance which is derived in [24], can be written as

$$\frac{\partial L(x)}{\partial x} = \frac{-K_a}{(K_b + x)^2} \tag{17}$$

Where K_a and K_b are constants and can be find by taking two specified force and stroke measurements. Plugging the preceding equation into Eq. (16) and by considering the relationship between power and current ($P = Ri^2$), the force-stroke relationship for the specified power will be obtained as

$$F = \frac{1}{2R} \frac{-K_a}{(K_b + x)^2} P \tag{18}$$

Where R is the coil resistance.

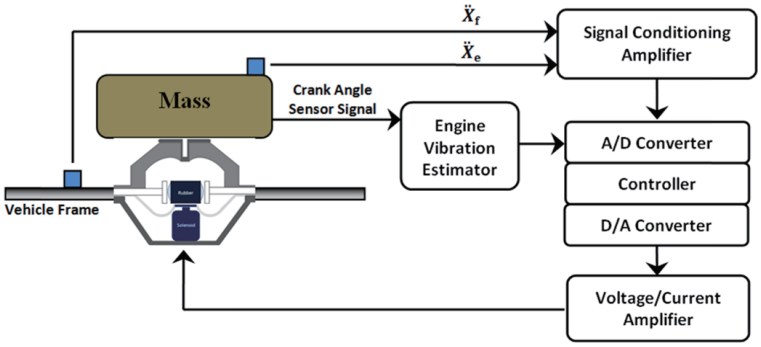

Fig. 13. Control system configuration.

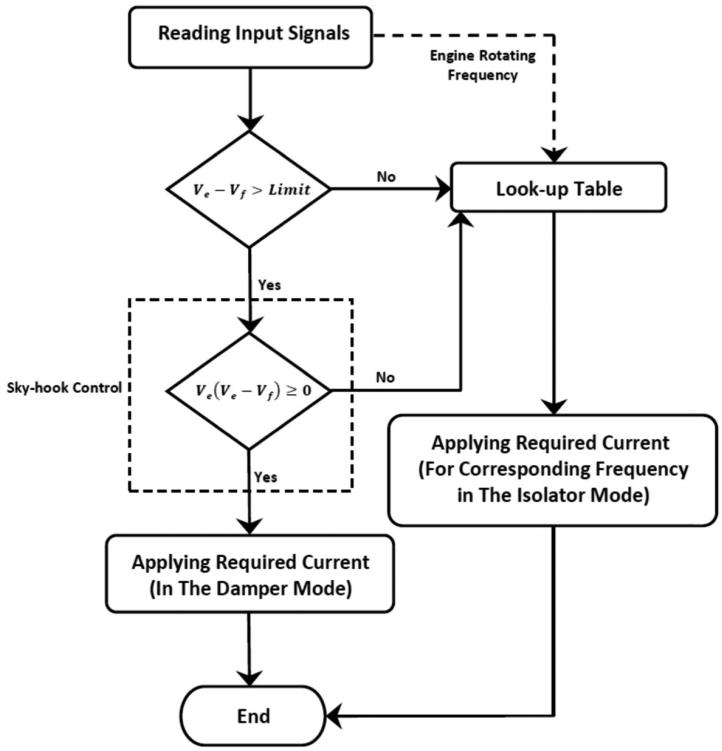

Fig. 14. Signal flows of the proposed controller.

The commercial linear solenoid is selected and by taking two specified force and stroke measurement, the force-stroke relationship obtained for a power in continuous operation mode (41 watts) and also in 10% duty cycle mode (410 watts). Figure 12 shows the force-stroke relationship. It must be mentioned that the graph is based on assumptions mentioned in theory section. It must be noted that beside the good performance of the proposed mount in reducing the transmitted force to the frame, the required power for this mount is more than the required power for a magneto-rheological hydraulic mount.

8. Control strategy considerations

Based on the observed response of the mount, a proper controller can be designed. In this design, the control is based on the engine rotation frequency and also accelerations of the engine and the vehicle frame. The former is

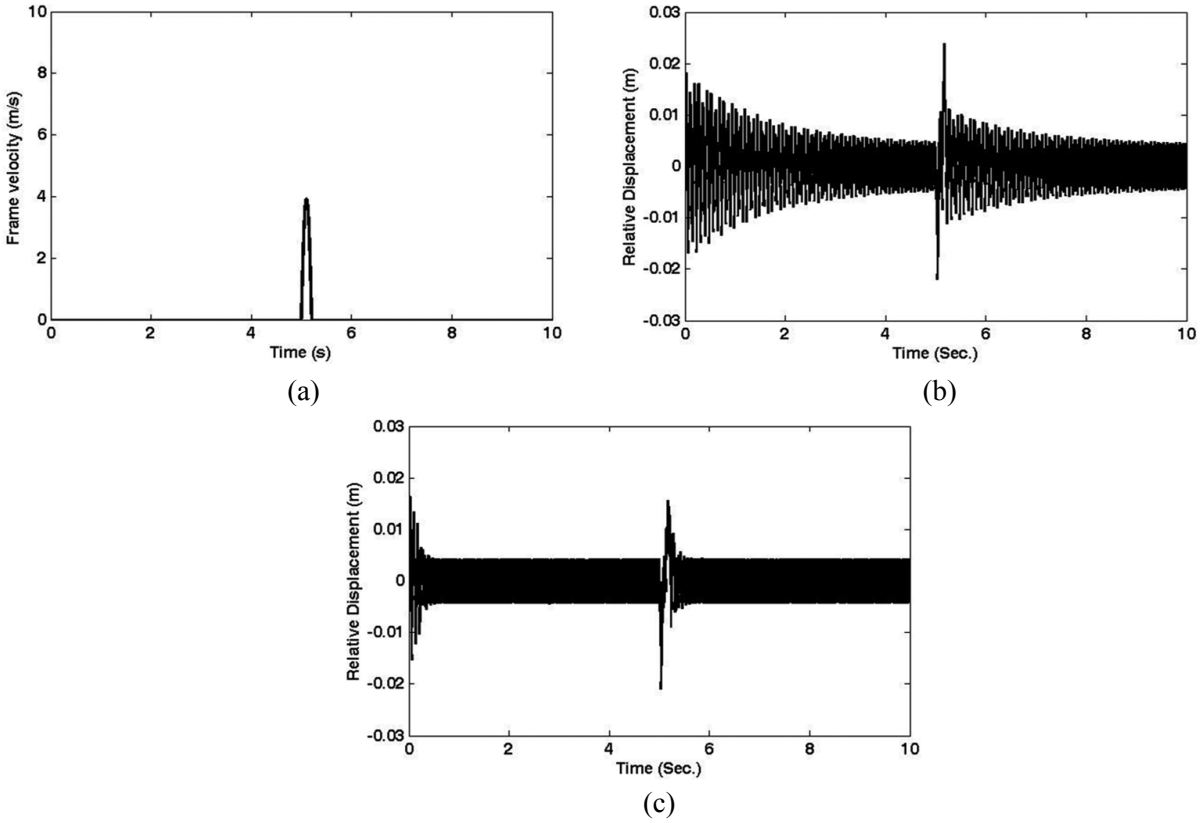

Fig. 15. (a) Frame velocity input, (b) Relative displacement between engine and frame in the passive mode, (c) Relative displacement between engine and the frame in the semi-active mode.

measured by a tachometer and the later is measured by two accelerometers mounted on the engine and the frame, respectively. Figure 13 shows the proposed control system. The diagram shown in Fig. 14 explains the signal flows for the proposed controller.

Engine frequency will be used as input to the control system to adopt the mount in the isolation mode and to achieve best reduction of the transmitted force.

Practical sky-hook configuration [25] has been used in the control algorithm that could shape the dynamic of the hydraulic mount in the damper mode (when the relative velocity between engine and frame exceed the limit).

To evaluate the dynamic performance of the proposed mount and the control strategy, some simulations were carried out. In the first simulation, the performance of the mount in controlling the relative displacement between the engine and the frame is conducted. Figure 15(a) displays the frame velocity when experiencing a bump in the road. Figures 15(b) and 15(c) demonstrate the relative displacement between the engine and the frame. A better relative displacement reduction can be seen in the semi-active mode.

In the second simulation the engine with variable rotation frequency is considered. Figure 16(a) shows the change of engine frequency versus time in this simulation. Figures 16(b) and 16(c) demonstrate the transmitted force to the frame resulting from the engine unbalance frequency in the passive and semi-active system, respectively. It is clear that the semi-active system can reduce the transmitted force wildly in the proposed frequency range.

9. Conclusions

In this paper, a new semi-active hydraulic mount design has been presented which provides variable notch frequency location regarding to engine speed in the highway driving condition and also can be converted to a damper

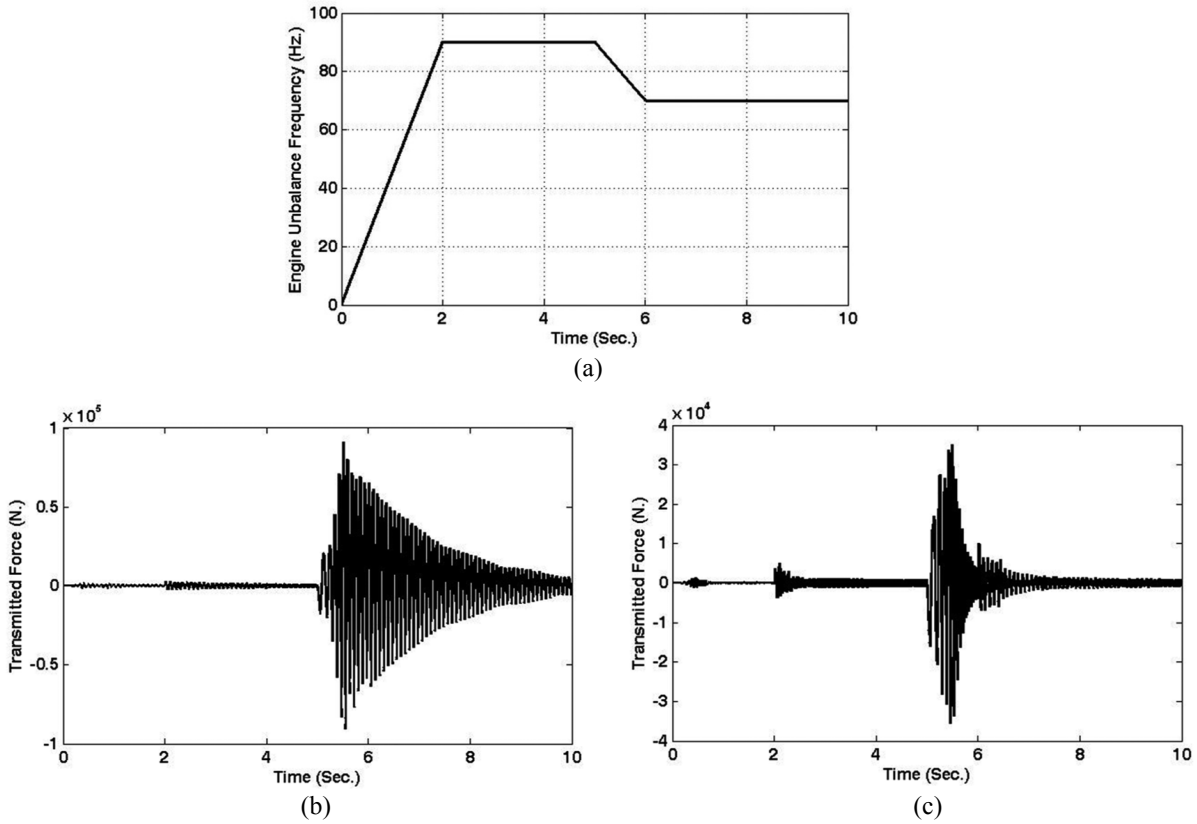

Fig. 16. (a) Engine rotational frequency, (b) Transmitted force in the passive mode, (c) Transmitted force after implementing control strategy.

when needed. The new design was described and its mathematical model was presented. It was shown that the new design can provide vibration and noise isolation at a wide range of frequencies; also, one can converted it to a damper by applying required force. To control the proposed hydraulic engine mount, a control strategy was suggested that adjust the input force to the rubber disk to achieve best vibration isolation in two-mode operation meaning isolating mode in the highway driving condition and damping mode in the shock motions.

References

[1] Y.K. Ahn et al., Optimal design of an engine mount using an enhanced genetic algorithm with simplex method, *Vehicle System Dynamics* **43**(1) (2005), 57–81.
[2] G.N. Jazar and F. Golnaraghi, Engine mounts for automotive applications: A survey, *The Shock and Vibration Digest* **34**(5) (2002), 363–379.
[3] G. Kim and R. Singh, A study of passive and adaptive hydraulic engine mount systems with emphasis on non-linear characteristics, *Journal of Sound and Vibration* **179**(3) (1995), 427–453.
[4] D.E. Barber and J.D. Carlson, Performance characteristics of prototype MR engine mounts containing LORD glycol MR fluids, *Journal of Physics: Conference Series* **149**(1) (2009), 012035.
[5] M. Ahmadian and Y.K. Ahn, Performance analysis of Magneto-Rheological mounts, *Journal of Intelligent Material Systems and Structures* **10**(3) (1999), 248–256.
[6] N. Vahdati and M. Ahmadian, Variable volumetric stiffness fluid mount design, *Shock and Vibration* **11**(1) (2004), 21–32.
[7] S.-B.S. Choi and H.-J.H. Song, Vibration control of a passenger vehicle utilizing a semi-active ER Engine mount, *Vehicle System Dynamics* **37**(3) (2002), 193–216.
[8] S.R. Hong et al., Vibration Isolation of Structural Systems Using Squeeze Mode ER Mounts, *Journal of Intelligent Material Systems and Structures* **13**(7–8) (2002), 421–424.
[9] T. Ushijima, K. Takano and T. Nojuchi, Rheological Characteristics of ER Fluids and Their Application to Anti-Vibration Devices with Control Mechanism for Automobiles. SAE Paper # 881787, 1988.

[10] D.E. Barber and J.D. Carlson, Performance characteristics of prototype MR engine mounts containing glycol MR fluids, *Journal of Intelligent Material Systems and Structures* **21**(15) (2010), 1509–1516.
[11] S.B. Choi et al., Vibration control of a passenger vehicle featuring magnetorheological engine mounts, *International journal of Vehicle Design* **33**(1) (2003), 2–16.
[12] M.S. Foumani, A. Khajepour and M. Durali, Application of shape memory alloys to a new adaptive hydraulic mount, SAE paper, 2002, pp. 2002-01-2163.
[13] M.S. Foumani, A. Khajepour and M. Durali, A new high-performance adaptive engine mount, *JVC/Journal of Vibration and Control* **10**(1) (2004), 39–54.
[14] T.Q. Truong and K.K. Ahn, A new type of semi-active hydraulic engine mount using controllable area of inertia track, *Journal of Sound and Vibration* **329**(3) (2010), 247–260.
[15] Y.Q. Zhang and W.B. Shangguan, A novel approach for lower frequency performance design of hydraulic engine mounts, *Comput Struct* **84**(8–9) (2006), 572–584.
[16] S. Arzanpour and M.F. Golnaraghi, A novel semi-active magnetorheological bushing design for variable displacement engines, *Journal of Intelligent Material Systems and Structures* **19**(9) (2008), 989–1003.
[17] N. Vahdati and M. Ahmadian, Single Pumper Semi-Active Fluid Mount, in *ASME Conference Proceedings*, 2003: ASME.
[18] N. Vahdati, A detailed mechanical model of a double pumper fluid mount, *Journal of Vibration and Acoustics, Transactions of the ASME* **120**(2) (1998), 361–370.
[19] S. Pinarbasi, U. Akyuz and Y. Mengi, A new formulation for the analysis of elastic layers bonded to rigid surfaces, *International Journal of Solids and Structures* **43**(14–15) (2006), 4271–4296.
[20] S. Pinarbasi, Y. Mengi and U. Akyuz, Compression of solid and annular circular discs bonded to rigid surfaces, *International Journal of Solids and Structures* **45**(16) (2008), 4543–4561.
[21] R.L. Wood and K.L. Lawrence, Modeling and Simulation of Dynamic Systems, 1997, University of Texas at Arlington: Prentice Hall.
[22] Y. Yu et al., Automotive Vehicle Engine Mounting Systems: A Survey, *Journal of Dynamic Systems, Measurement, and Control* **123** (2001), 186–194.
[23] E.E. Ungar and D. Ross, Vibrations and noise due to piston-slap in reciprocating machinery, *Journal of Sound and Vibration* **2**(2) (1965), 132–146.
[24] S.E. Lyshevski, *Electromechanical Systems, Electric Machines, and Applied Mechatronics electric Power Engineering Series*, 1999, New York: USA CRC Press.
[25] M. Ahmadian and C.A. Pare, A Quarter-Car Experimental Analysis of Alternative Semiactive Control Methods, *Journal of Intelligent Material Systems and Structures* **11**(8) (2000), 604–612.